# Using ABAQUS with 3D imaging techniques for material characterization

A. Abdul-Aziz[1], G. Limbert[2], P.G. Young[3], T. Beresford-West[4]

[1]Nasa Glenn Research Center, USA
[2]First Numerics, UK
[3]School of Engineering, Computer Science and Mathematics, University of Exeter, UK
[4]Simpleware Ltd, UK

*Abstract: Image-based meshing is opening up exciting new possibilities for the application of computational continuum mechanics methods (e.g. CFD and FEA) to material characterization based on micro-structural scan data. An innovative mesh generation technique has been developed which converts 3D scanner data (such as from microCT or X-ray tomography) directly into meshes suitable for use in FE and CFD simulations. The ease and robustness with which simulation models can be generated have opening up exciting new avenues in materials research, particularly in materials characterization and non destructive testing. The approach has several key advantages including: i) Multi-part meshing: the ability to generate robustly meshes for topologies of arbitrary complexity (such as composites or foams) and with any number of constituent materials; ii) Image-based accuracy: the geometric accuracy of mesh domains is only dependent on image accuracy; iii) The ability to assign material properties within a given structure based on signal strength, for example based on cell density.*

*A range of case studies solved using ABAQUS CAE will demonstrate the potential of the proposed approach for exploring micro to macro-scale properties, and illustrates the ability to complete such complex problems with a high degree of accuracy but in a fraction of the time taken by other approximate approaches.*

*Keywords: Non destructive testing, Finite Element, Image based meshing, Material characterisation, 3D imaging.*

## 1. Introduction

Although 3D imaging techniques (such as MRI, CT and Micro-CT) were initially developed for the medical field they have in recent years increasingly been adopted in the materials research field for qualitative and semi-quantitative characterisation of the micro-structural behaviour of a range of natural and man-made materials. More recently the use of these images as the basis for generating finite element and CFD models for use in physics based simulations has gained ground (Watson et al. 2006, Abdul-Aziz et al. 2006, Berre et al. 2006).

Most approaches mooted to date for generating 3D volume meshes have involved an intermediary step of surface reconstruction followed by the use of traditional CAD based meshing algorithms. However this fails to exploit the fact that in image based meshing, unlike for CAD based meshing, surfaces are not explicitly defined but only implicitly as the surface boundaries of a segmented volume of interest. Exploiting this difference leads to a far more accurate, robust and direct approach which combines the geometric detection and mesh creation stages in one process. In this paper we use a methodology that generates 3D hexahedral or tetrahedral cells throughout the volume of the domain, thus creating the mesh directly. This technique was originally developed for FE analysis of bones, for both stress and vibration analysis, and has been implemented as a set of computer codes (ScanIP, $^{+}$ScanFE). Since FE and FV meshes are conjugate structures, the same techniques can be used to output a FV mesh (cell/face representation, rather than point/edge representation).

The process of generating a mesh involves first segmenting the different volumes of interest (VOI) from the 3D data. Both semi-automated and manual techniques are available within ScanIP, as well as a range of alternative image processing packages, to provide segmented masks. Techniques include noise filters, three dimensional thresholding tools through to bitmap painting. These VOI are then simultaneously meshed based on an orthotropic grid intersected by interfaces defining the boundaries. In effect a base Cartesian mesh of the whole volume defined by the sampling rate is tetrahedralised at boundary interfaces based on cutting planes defined by interpolation points. Smooth boundaries are obtained by adjusting the interpolation points in one, or a combination, of two ways: by setting points to reflect partial volumes or by applying a multiple material anti-aliasing scheme. The process results in either a mixed tetrahedral/hexahedral mesh or a pure tetrahedral mesh and incorporates an adaptive meshing scheme.

The adaptive meshing scheme preserves the topology but reduces the mesh density where possible towards the interior of the mesh by agglomerating hexahedra into larger hexahedra and generating transitional tetrahedra.

The approach is fully automated and robust creating smooth meshes with low element distortions regardless of the complexity of the segmented data. The approach adopted allows for an arbitrary number of different VOI to be meshed. As neighbouring sub-meshes share a common cutting surface, this ensures a node to node correspondence at the boundaries between different meshed volumes, thus trivially satisfying the geometrical constraints at the boundary (in other word no gaps or overlaps). In addition the numbering scheme will be the same for the mesh interface as seen from either side - a topological requirement on the meshes. This is also easily fulfilled using our approach.

The use of these meshing techniques as the basis for both structural and hydro-dynamic analysis of architectures of extremely complex topology is illustrated by exploring the behaviour of auxetic foam based on high resolution image data.

## 2. Case study – Auxetic foam

### 2.1 Auxetic material

Auxetic foam materials (Figure 1) are used in a variety of industrial applications (sound and shock absorption) and are very promising for novel applications in medical engineering. By actively controlling their microstructure through specific loading conditions they can allow/prevent fluid and solid particles flow in specific directions. Thanks to this useful characteristic, auxetic foams can be used as tuneable filters for filtration of biological fluids and/or process engineering.

**Figure 1. Scaled rapid-prototyping model of an auxetic foam sample [real dimensions: 0.1 x 0.1 x 0.1 mm].**

Auxetic materials have the particular property of expanding in all directions when stretched in one direction thus exhibiting a negative Poisson's ratio. Similarly, a sample of auxetic material submitted to compression in one direction will contract in the other directions. This counter-intuitive behaviour stems from the unusual micro-architecture of these materials. Other significant structural properties include increased shear stiffness, increased plane strain fracture toughness and increased indentation resistance.

There is therefore a real industrial need for understanding, developing and predicting the mechanical and hydrodynamic behaviour of auxetic materials. Predicting accurately the physical properties of auxetic materials is difficult with analytical methods and the stochastic nature observed in manufactured auxetic foams can only be accurately modelled using computational mechanics simulations. The authors will here investigate the microstructural property of an industrial auxetic foam.

High-resolution 3D scan data of open celled foam was obtained and the data was straightforwardly segmented using threshold and floodfill tools in ScanIP. A 3D smooth volumetric mesh was generated within +ScanFE. The total combined image processing and meshing time, including user interaction time, was less than 20 minutes.

### 2.2 Mesh generation

High-resolution three-dimensional scan data of the auxetic foam sample were obtained from synchrotron scanning facilities at the Advanced Photon Source at Argonne National Laboratory, IL,USA (courtesy of Dr. Jerry Seidler, University of Washington, Seattle, USA), processed and automatically converted to a three-dimensional finite element mesh.

The total combined image processing and meshing time, including user interaction time, was less than ten minutes on a 2 GHz Pentium PC. The finite element mesh generated by the software module +ScanFE consisted of very large number of elements (about 620,000). Figure 2 presents an enlarged view of the finite element mesh which highlights the complex structural features of the auxetic foam.

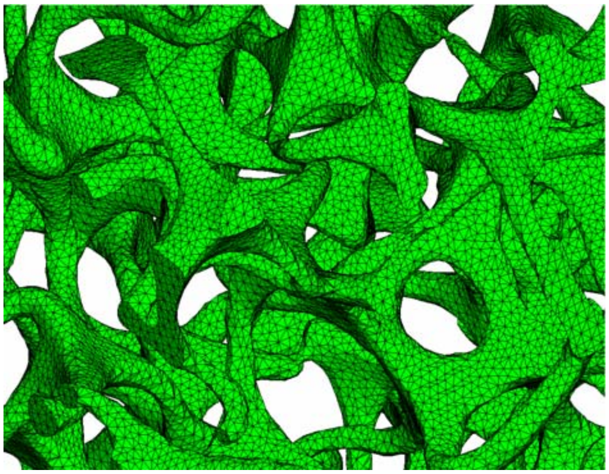

**Figure 2. Zoom-in view of the finite element mesh of the auxetic foam sample. Finite volume is simply dual of this mesh.**

### 2.3 Micro-structural analysis: FE analysis in ABAQUS

A non-linear finite element analysis was then performed using the software package ABAQUS to simulate large strain deformation. The finite element analysis simulating compression (about 30 % strain) of the auxetic foam took over 6.5 hours on a dual Intel Xeon processor PC cadenced at 2.8 Ghz but using a single processor.

The analysis demonstrated the negative Poisson's ratio effect. The auxetic structure collapsed towards its centre resulting in a lateral contraction as the vertical displacement of the top of the cube progressed. Figure 3 displays the fringe plot of the maximal principal compressive strains at various stages of the analysis. The numerous branching substructures of the auxetic sample lead to complex load redistribution patterns which affect the global deformation of the whole structure.

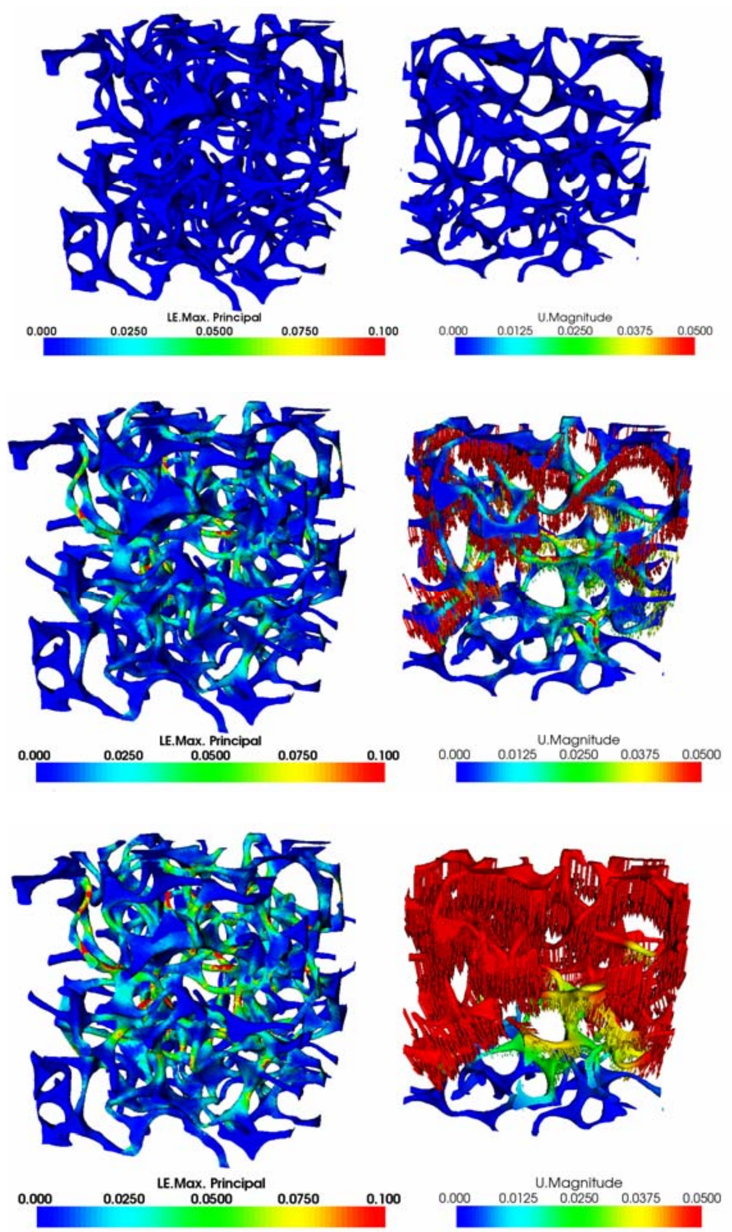


**Figure 3. Left: Maximal principal compressive strains (logarithmic strains plotted on undeformed configuration), Right: Displacement vectors at various stages of the deformation of the auxetic foam sample (a/: beginning of the analysis, b / increment 30, c/ increment 45, d/ increment 60, e/ increment 75: end of the analysis).**

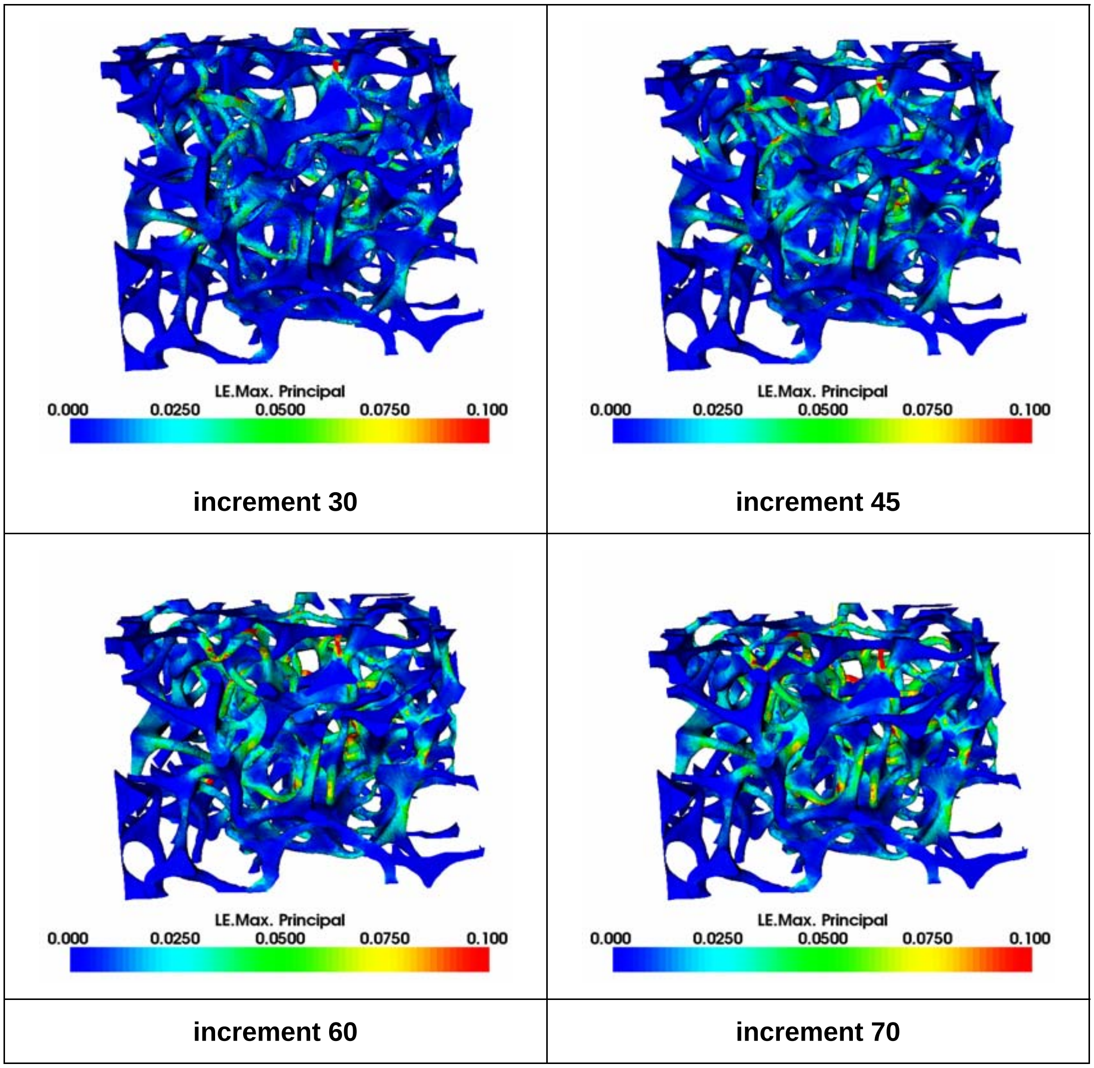


**Figure 4. Maximal principal strains (logarithmic strains) at various stages of the deformation of the auxetic foam sample (increment 0: beginning of the analysis / increment 86: end of the analysis).**

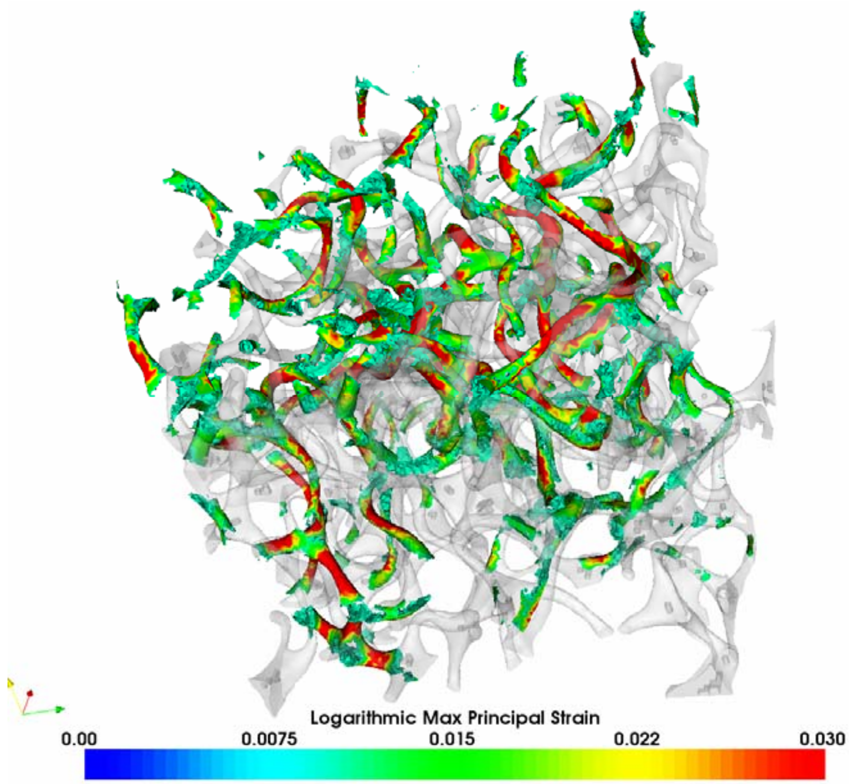


**Figure 5. Maximal principal strains (logarithmic strains) larger than 0.01 plotted on the undeformed configuration.**

## 3. Case study – Ceramic Matrix Composite

### 3.1 Specimen

The test specimen studied here consists of 40% Sylarmic fiber, 6-7% porosity, Boron Nitride (BN) internal coating, 20-25% Chemical Vapor Infiltrated (CVI)-SiC coating, and the rest is Melted Infiltrate (MI) matrix. Dimension of the test specimen are clearly shown in Figure 2. Additional details about the specimen materials characteristics and testing performed can be found in reference (Abdul-Aziz et al. 2002).

### 3.2 Image processing and Finite Element (FE) mesh generation

The process of constructing an accurate 3-D volume requires a series of 2-D CT slices of the specimen under consideration. For a detailed analysis, 2-D slices of around 0.2 mm are required, given the accuracy of the CT system used in this study. While such detail provides an accurate 3-D rendering of the whole internal volume, 0.2 mm spacing will create a cumbersome data base for manipulation. In this study, 20 slices were used. Each slices being a TIFF image of 1200x700 pixels. The in-plane resolution of the scanner was 0.2mm (in both X and Y directions), whereas the separation between each slice was 1.25 mm.

### 3.3 Cropping

The data originally contained more space then the specimen actually occupies. A cropping was therefore performed, in order to only preserve the extents of the data containing the specimen. This resulted in a smaller 697x211x20 volume, close tight to the data.

### 3.4 Filtering

Due to the noisy nature of the image, some filtering was necessary. The Curvature Anisotropic Diffusion filter, offered by ScanIP was therefore used. It should be noted that it is considered as a Noise Reduction filter, rather than a Smoothing filter, the reason being that its purpose is to reduce noise while preserving features, which is not the case of smoothing filters such as Gaussian filtering. Curvature Anisotropic Diffusion filter was applied with a conductance of 5, a time step of 0.0625, and 10 iterations.

### 3.5 Image Segmentation

Segmentation is the process of identifying, within an image, what pixels belong to each object of interest. In this study, a total of 10 Finite Element (FE) models were considered, differing by mesh density, geometrical definition, or by the way material properties are defined. The segmentation process itself only influences the geometrical definition of each model, and there are actually 4 models that are geometrically different. Pixels of values ranging from 121 to 255 were thresholded to create a part representing the matrix.

### 3.6 Mesh generation

[+]ScanFE was further used to generate a number of finite element meshes based on the 3-D segmented image data. The density of meshes generated in ScanFE is closely connected to image resolution so in order to explore convergence of results (field parameters of interest), the image was downsampled to create two volumes of 139x42x24 and 67x20x11 in order to generate, respectively, high and low resolution models. An interesting point can be made here about image based models versus CAD models. Unlike CAD models where the geometry of the model is assumed to be exact and mesh density is increased principally in order to obtain a better model of the field parameters of interest (say the stress field within a loaded structure), with image based models both the response and the geometry of the system are approximated. By generating models based on increasing image resolutions one not only improves the modeling of the response but also the representation of the geometry (one effectively converges to the geometry). Hence one can perform essentially dual or coupled convergence study; This type of study provides powerful arguments for the validity of the simulations as convergence of results demonstrates not only that the mesh is of sufficient density to capture the field parameter of interest but also, and as importantly, that the image resolution on which the model is based is high enough to capture relevant features in the scanned object.

Ten models were generated within +ScanFE using 20 iterations of ScanIP's proprietary multipart anti-aliasing algorithm, followed by 2 iterations of Laplacian smoothing. The anti-aliasing (aa) techniques implemented ensure high accuracy of reconstruction; unlike many smoothing schemes they are volume, topology and geometry preserving ensuring models whose geometric accuracy is contingent only on image quality (on the accuracy of the segmentation). Mesh optimization parameters ensured that the element quality index reached a value of 0.15, allowing off surface nodes (within a pixel distance). Figure 4 shows a model which represents a view of the mesh and the internal features illustrating various anomalies within the ceramic materials.

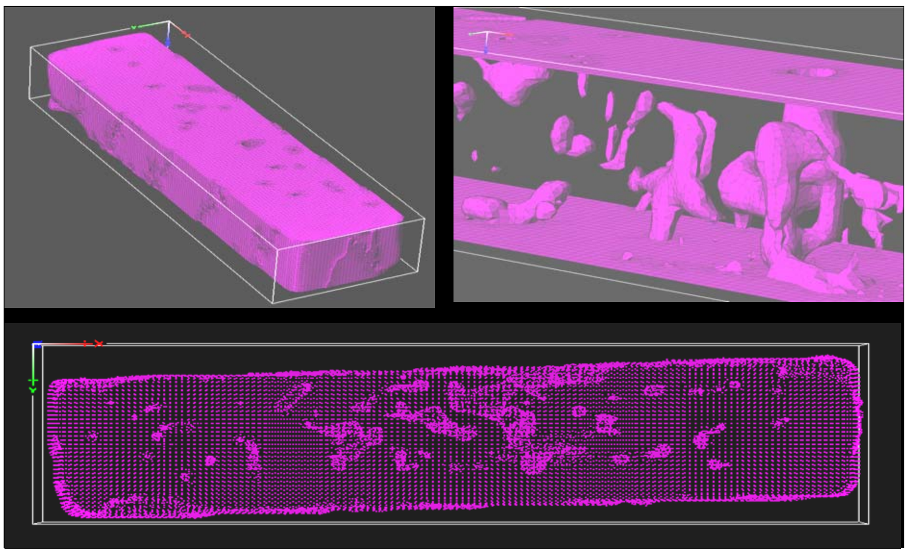

**Figure 6. General view (upper left), detail of holes (upper right), and point cloud view (bottom).**

### 3.7 Finite Element Analysis in ABAQUS

Finite element analyses were carried out using ABAQUS. All the analytical calculations were performed under linear elastic condition and orthotropic material provision. The Boundary conditions were implemented such that on one side all the nodes were restrained from movement along the symmetry-axis, and on the opposite side, the middle nodes along both the X-axis and the Y-axis were restrained from moving in the X and Y-directions respectively, see Figure 5. This arrangement offered a reasonable simulation to the gripping conditions imposed during testing. Axial loading was applied accordingly. It should be noted that displacement boundary conditions in front of the block were invoked such as all the nodes are coupled to move together

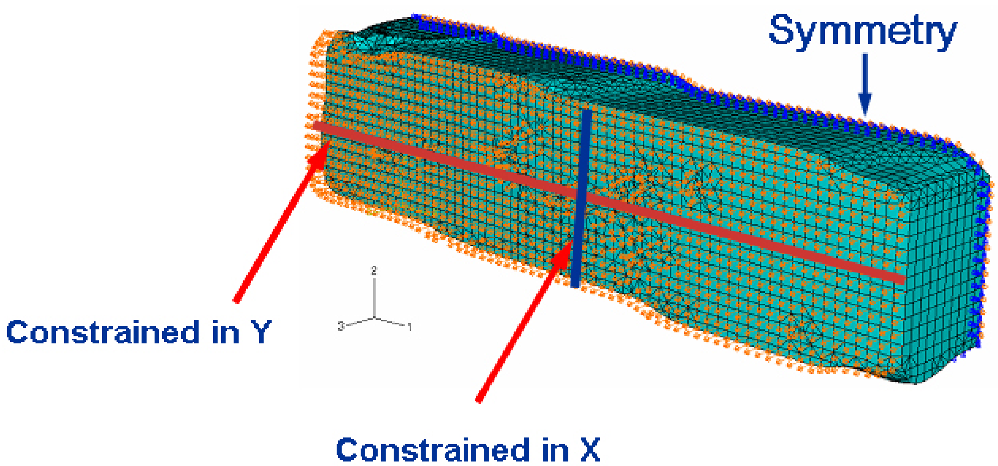


**Figure 7. Finite element model of the specimen test section showing applied boundary conditions.**

### 3.8 Results

Sample results for a high resolution reconstruction of the image which includes voids and material anisotropy are shown. Results below for selected cases show deformation under an applied tensile strain from which the effective Young's modulus of the specimen was obtained. Also peak stress concentration and hence areas of potential failure through crack initiation can be identified. A key advantage is having a skill to carry out experimental studies in parallel with analytical ones on the actual sample scanned and be able to better explore stability and failure mechanisms.

A number of different models and simulations were carried out in order to explore the sensitivity of numerical predictions to a range of modelling assumptions including:

- Modelling versus ignoring voids – In this case because of the relatively low porosity this had reasonably small effect on effective Young's modulus but very large effect on peak stresses predicted and hence prediction of onset of failure.
- Modelling voids explicitly versus. simplified representation of voids as areas of very low stiffness.
- Influence of assumed threshold on predicted stresses- this is seen as quite a critical parameter as predicted stresses are at this level of representation of complex geometries of the holes very sensitive to accurate representation of morphology. Nonetheless a qualitative understanding of possible weakening of the structure can be gauged from numerical studies.

A wide range of analyses were carried out to explore the sensitivity of numerical predictions to a range of parameters including mesh density and segmentation parameters. The work shows that new image based meshing techniques can provide a robust and turnkey approach to the understanding of the influence of microstructural characteristics on macro structural (bulk) properties of complex composites.

Increasing mesh density provides not only better representation of field parameter of interest but also better geometric representation of the problem. The predicted effective modulus was relatively insensitive to mesh density however the peak stresses observed within the matrix (at stress concentration points caused by holes) was, as can be expected, quite sensitive.

## 4. Conclusions

Automated mesh construction from 3D imaging is one of the most interesting new developments in computational mechanics. Because of their inherent geometrical complexity, the construction of even generic models of typical micro-structures is time-consuming and potentially inaccurate. Most previous approaches to this problem have concentrated on generating surface representations for the outer boundary and have left the mesh generation as a separate step. In contrast, our approach has been to generate the mesh directly from 3D images as part of the image analysis process. This approach leads to simpler and more robust multi-part meshes which are suitable for modelling using a range of different physics based simulation methods including for coupled fluid structure interaction (FSI) problems. In addition, the accuracy of models generated is contingent only on the accuracy of the original imaging data providing the most faithful and realistic models possible from the image data.

The present study illustrates the ease with which FE and FV models of microstructures of arbitrarily complex topology created based on 3D tomographic images (MicroCT) can be straightforwardly generated and used to carry out (large deformation) compression simulations using ABAQUS and flow analyses using FLUENT. This shows the potential of image based meshing techniques coupled with physics based simulation tools to provide accurate, fast, robust and practical tools to explore the bulk structural properties of foams and composites materials based on micro-structural data. Future studies will explore comparing quantitative data obtained from experimental, analytical and numerical analyses.

## 5. References


1. Abdul-Aziz, A., Baaklini, Y.G., Bhatt, R.T., “Non Destructive Evaluation Of Ceramic Matrix Composites Coupled With Finite Element Analyses”, 7th International Symposium on Nondestructive Evaluation and Health Monitoring of Aging Infrastructure, 17-21 March 2002 San Diego. Bellingham: SPIE, 2002.
2. Abdul-Aziz, A., Saury, C., Bui Xuan, V., Young, P., “On the material characterization of a composite using micro CT image based finite element modelling”, Smart Structures and Materials and NDE, 26 February-2 March 2006 San Diego. Bellingham: SPIE, 2006.
3. Berre, C., Fok, S.L., Marsden, B.J., Babout, L., Hodgkins, A., Marrow, T.J., Mummery, P.M., “Numerical modelling of the effects of porosity changes on the mechanical properties of nuclear graphite”, Journal of Nuclear Materials, 352, 1-5, 2006.

4. ScanIP and +ScanFE software developed by Simpleware Ltd, Innovation Centre, Rennes Drive, Exeter EX4 4RN, UK. http://www.simpelware.com
5. Watson, I.G., Lee, P.D., Dashwood, R.J., Young, P., "Simulation of the Mechanical Properties of an Aluminum Matrix Composite using X-ray Microtomography", Metallurgical and Materials Transactions A, 37A, 551-558, 2006.